THE DIFFUSE COSMIC X–RAY (>15 KEV) BACKGROUND WITH THE PDS INSTRUMENT ABOARD *BEPPOSAX*

F. Frontera[1,2], M. Orlandini[1], R. Landi[1], L. Amati[1], E. Costa[3], N. Masetti[1], and E. Palazzi[1]

[1]*INAF/Istituto di Astrofisica Spaziale e Fisica Cosmica, Bologna, Via Gobetti 101, 40129 Bologna, Italy*
[2]*Dipartimento di Fisica, Università di Ferrara, Via Saragat, 1, 44100 Ferrara, Italy*
[3]*INAF/Istituto di Astrofisica Spaziale e Fisica Cosmica, Roma, Via del Fosso del Cavaliere 100, 00133 Roma, Italy*

ABSTRACT

We report a new measurement of the hard (15–50 keV) Cosmic X–ray Background (CXB) after the last performed with the *High Energy Astronomical Observatory* (*HEAO–1*) in the late 1970s. Our measurement is performed with the PDS instrument aboard the *BeppoSAX* satellite. After the recently reported 2–10 keV CXB measurements obtained with the imaging instruments aboard the X–ray satellites *BeppoSAX*, *XMM-Newton*, and *Chandra* that give CXB intensities systematically higher than those obtained with *HEAO–1* in the same energy band, suspects of systematic errors in the *HEAO–1* measurements at low and higher energies have been raised by several authors. Using the *BeppoSAX* PDS pointings at high galactic latitude ($|b| > 15^{\circ}$) we have measured the CXB spectrum and intensity level in the 15–50 keV energy band. Our results are consistent with those obtained with *HEAO–1* at the same energies.

Key words: X–rays: diffuse background — cosmology: diffuse radiation — cosmology: observations.

1. INTRODUCTION

The origin of the Cosmic diffuse X–ray Background (CXB) after more than 40 years from its discovery [1] still remains one of the most fascinating issues. Actually at energies less than 10 keV the situation is being clarified: thanks to various sky surveys, such as the 0.5–2 keV *ROSAT* satellite survey [2], the 0.5–10 keV *XMM-Newton* deep survey [3] and the *Chandra* Deep Fields North and South [CDF-N and CDF-S, 4, 5, 6, 7] it appears that, in the 0.5–8 keV band, from 70% to 90% of the CXB is resolved into discrete sources, mainly Active Galactic Nuclei (AGNs). This result could imply that also at hard X-ray energies (>10 keV), where the instrument sensitivity is much lower than that required, the CXB could be also resolved into point sources [see, e.g., 8], which are now impossible to single out but that they could be detected when new missions with focusing telescopes, now under development, will be launched.

However the ultimate answer about the nature of the CXB, either at high (>10 keV) or at low (<10 keV) energies, depends on the accuracy with which the CXB intensity is measured. Indeed, in spite of the fact that the CXB was discovered more than 40 years ago, its intensity is still not well known both at low and at high energies.

After the first pioneer measurements of the CXB spectrum, that showed the difficulty of performing an unbiased estimate of the CXB [for a review see 9], the major effort performed to get a reliable estimate of the CXB spectrum in a broad energy band starting from a few keV was done in the late 1970's with the A2 and A4 instruments aboard the *High Energy Astronomical Observatory 1* (*HEAO–1*). The CXB spectrum measured with A2 in the 3–60 keV energy band was first reported by Marshall et al. [10, hereafter M80] and later by Boldt [11, 12, 13, 14]. The results reported by M80 gave rise to a high excitation in the astrophysics community: the best fit to the data was a thermal bremsstrahlung, which was interpreted as due to emission from a hot diffuse intergalactic medium with an electron temperature $kT_e \approx 40$ keV, which could solve the dark matter issue. However this interpretation was not confirmed by the *Cosmic Microwave Background Explorer* (*COBE*): the presence of a truly diffuse hot plasma would produce a severe Compton distortion of the Cosmic Microwave Background (CMB), which was not observed by *COBE* [15]. The 13–180 keV CXB spectrum obtained with the *HEAO–1* A4 Low Energy Detectors (LED) was preliminary reported by Rothschild et al. [16] and Gruber [17], and finally by Gruber et al. (1999, thereafter G99), while that obtained with the *HEAO–1* Medium Energy Detectors (MED) in the 100–400 keV energy band was reported by Kinzer et al. [19]. G99 also performed a comparative analysis of the *HEAO–1* A2 and A4 results. Their conclusion was that all the *HEAO–1* results on the CXB spectrum are mutually consistent within their statistical and systematic uncertainties, with the best fit $E \times J(E)$ spectrum given by a bell shape with a maximum of 42.6 keV (cm^2 s keV)$^{-1}$ at 29.3 keV, and an energy spectrum below 60 keV given by a power–law with a high energy exponential cutoff (CUTOFFPL) $F(E) = 7.877E^{-0.29}\exp[-E/41.13]$ erg/(keV cm^2 s sr)$^{-1}$.

After the *HEAO–1* results, no other CXB measurement

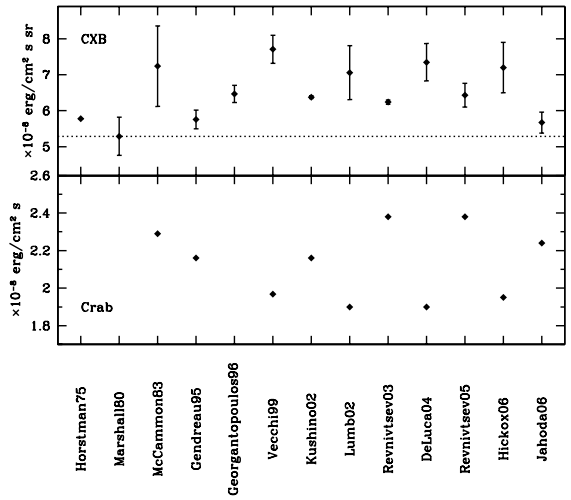

Figure 1. Upper panel: *Comparison of the 2–10 keV integral CXB intensities. The dotted line corresponds to the M80 value.* Bottom panel: *Corresponding 2–10 keV Crab fluxes used for flux scale calibration.*

was performed in the hard X–ray range (>15 keV), while at lower energies several CXB measurements were performed with imaging telescopes on board the satellite missions *ROSAT* [0.1–2 keV, 20], *ASCA* [1–8 keV, 21, 22], *BeppoSAX* [1–8 keV, 23], *XMM-Newton* [2–8 keV, 24, 25], *Chandra* [0.5–8 keV, 7], and with the non imaging *Proportional Counter Array* [PCA, 3–15 keV, 26] aboard the *Rossi X–ray Time Explorer* (*Rossi-XTE*) (see Fig. 1). The results of these measurements is that all the low energy measurements performed after that with *HEAO–1* show higher CXB intensities, even if they are not mutually consistent. The lowest values are those obtained with *ASCA* [21, 22] and with the RXTE/PCA by Revnivtsev et al. [26]. Regarding the latter measurement, the derived CXB intensity could be lowered from the quoted value (18% higher than *HEAO–1*) down to 6% higher than that by M80 by adopting a more appropriate calibration of the flux scale. Indeed their adopted instrument response function is calibrated on the Crab Nebula spectrum quoted by Zombeck [27] that predicts an unabsorbed 2–10 keV flux from Crab of 2.39×10^{-8} erg cm^{-2} s^{-1}, which is the highest of the estimated Crab fluxes: it is higher by $\sim$12% than the mean value of the fluxes measured with several other instruments (see Fig. 1). Using the lower flux scale, the CXB intensity is correspondingly lowered.

The 3–10 keV CXB intensity found by Revnivtsev et al. [28] from the re-analysis of a *HEAO–1* A2 data set is higher than that by M80 by about 20%. But, as also noticed by Jahoda et al. [29], who have performed the spectral analysis of the same data set used by Revnivtsev et al. [28] and quote a lower intensity value for the CXB intensity, a partial explanation of the discrepancy is due to the flux scale which was calibrated on the Crab spectrum given by Zombeck [27]. Thus, also in this case, the previous considerations hold and the CXB intensity reported by Revnivtsev et al. [28], can be reasonably lowered down to a value about 8% higher than that by M80 by a recalibration of the flux scale (see Fig. 1).

In spite of the discrepancies among the low energy measurements, several authors [e.g., 31, 32] consider the most recent results more reliable than those obtained with *HEAO–1* A2 in the same energy band [see, e.g., 25]. As a consequence, given that the model spectrum given by G99 is considered to be the likely shape of the true CXB spectrum, also the intensity level obtained with the *HEAO–1* A4 LED detectors, which was consistent with that of the A2 experiment, is expected to be underestimated. The CXB synthetic models are equally affected by these observational uncertainties, and favor the most recent CXB results. As an example, Comastri [8] assumes the analytical fit of G99 renormalized upward by a factor 1.3, and a similar renormalization is adopted by Ueda et al. [33].

Given the importance of the CXB normalization in order to establish the correct contribution of discrete sources to the CXB and the expected contribution of a yet undetected population of highly obscured sources and/or a diffuse component, we have derived an estimate of the high energy (>15 keV) CXB spectrum and its normalization exploiting the pointed observations performed with the *Phoswich Detection System* (PDS) aboard the *BeppoSAX* satellite. This is the first hard X–ray measurement of the CXB after that of *HEAO–1*.

2. THE INSTRUMENT

Even though the PDS was not designed to perform a spectral measurement of the CXB, *a posteriori* we became convinced that such measurement was possible with this instrument, given its very good performance in terms of stability, background level, calibration and flux sensitivity. The PDS [34] made use of 4 independent and equal detectors, each based on a sandwich of two optically coupled NaI(Tl) and CsI(Na) inorganic scintillators of 3 and 50 mm thickness, respectively, both viewed by a photomultiplier in which the NaI(Tl) had the role of main detector and the CsI(Na) that of active shield. Signals from each of the two detectors were recognized from their scintillation time constant (phoswich technique). This technique is one of the most effective techniques to perform an unbiased spectroscopy of the continuum emission and to minimize the intrinsic background. In order to further decrease the instrumental background, an active anticoincidence shield, made of 4 slabs of CsI(Na) scintillators were used. This shield was also used as Gamma Ray Burst Monitor, the well known GRBM on board *BeppoSAX* [34] that had a leading role, along with the Wide Field Cameras [35], for the discovery of the origin of GRBs [see, e.g., 36]. The gain of the detection units was continuously controlled and equalized to each other. The instrument FOV of 1.3° (FWHM) was obtained by means of two independent rocking collimators which alternated, with a default dwell time of 96 s, between the neutral po-

sition (ON source) and two symmetrical positions which were rotated with respect to the neutral position by $\pm 3.5^\circ$ ($\pm$OFF). The total detection area through the collimators was 640 cm^2. The high PDS sensitivity is mainly due to the excellent performance of the phoswich analysis system and anti-coincidence shields, combined with the almost equatorial *BeppoSAX* orbit (3.7° inclination), which allowed a radiation environment with a low level of high energy particles and radioactivity, in addition to a small change of the cutoff rigidity (10–16 GV) along the orbit, and a marginal entrance in the South Atlantic Geomagnetic Anomaly (SAGA) region.

The instrument background level was very low for the entire *BeppoSAX* life with an intensity $B(15\text{–}300\ \mathrm{keV}) = 1.6 \times 10^{-4}$ counts (cm^2 s keV)$^{-1}$ [36] at the beginning of the mission and a slow decrease with the decay of the orbit (Orlandini et al., in preparation). The 15–300 keV limit sensitivity corresponded to about 1% of the background level with a marginal influence of systematic errors in the background subtraction [37], thanks to its continuous monitoring with the rocking collimators.

The good spectral determination capabilities of PDS were also obtained thanks to the excellent performance of the phoswich electronics, as confirmed by the calibration results obtained with several repeated observations of the Crab Nebula. Assuming a power–law (PL) model, the photon index Γ remained unchanged within the statistical uncertainties for the entire *BeppoSAX* life time, with a mean value of 2.121 ± 0.001. We notice however that the best fit of the 15–200 keV count rate spectrum of Crab was obtained with a broken power–law (BKNPL), with a mean low energy index $\Gamma_1 = 2.113 \pm 0.001$, a break energy $E_\mathrm{b} = 74 \pm 2$ keV, and a high energy index $\Gamma_2 = 2.198 \pm 0.005$, consistent with other measurements [see, e.g., 38]. The cross-calibration of the PDS with the MECS telescope on board *BeppoSAX*, performed with Crab, has provided a mean normalization ratio between PDS and MECS of $R(\mathrm{PDS/MECS}) = 0.928 \pm 0.001$ in the assumption of a PL model, and 0.917 ± 0.001 in the assumption of a BKNPL.

A comparison of the PDS spectrum with that obtained with other instruments has shown that the 15–60 keV flux from the Crab, when corrected for the above normalization ratio $R(\mathrm{PDS/MECS})$, is consistent within 4% with both the extrapolation of the recent 0.3–10 keV spectrum obtained with *XMM-Newton* [39], and the classical Toor and Seward [40] results. Within 10%, it is also consistent with the 20–1000 keV spectral measurement performed with the GRIS balloon experiment [38].

3. THE MEASUREMENT METHOD OF THE UNRESOLVED CXB

The measurement of the unresolved CXB requires the knowledge of the instrument intrinsic background level ν_{in} to be subtracted to the total background level ν_B^{sky} measured during the observation of a blank sky field (the latter is expected to be given by the sum of the CXB count rate ν_{CXB} plus ν_{in}). Thus an unbiased measurement of ν_{CXB} is not an easy task, given that systematic errors intervene due to either a biased selection of blank fields or a wrong ν_{in} evaluation or both.

In the case of the *HEAO–1* A2 experiment, the 3–60 keV spectrum was obtained by comparing, for each of three X–ray similar detectors, the total background levels simultaneously observed through two collimators, one with a solid angle twice that of the other. Assuming ν_{in} to be independent of the instrument FOV, the difference between the two total background levels removes the intrinsic background and gives directly ν_{CXB} (M80). In the case of the *HEAO–1* A4 experiment which included both low energy (LED, 13–180 keV) and a high energy (HED, 100–400 keV) detectors, the CXB estimate was obtained by subtracting from the total background ν_B measured when the detectors observed blank sky fields the background measured when the FOV of the detectors was shielded with a shutter of scintillating material put in anti-coincidence with the main detectors [18, 19]. In both cases, a systematic error in the ν_{CXB} estimate cannot be excluded given that the intrinsic background is mass-dependent. Indeed, in the former case, detectors of different collimator apertures can have a different ν_{in}, while, in the latter case, the shutter can modify the intrinsic background due the possible presence of events which are not anti-coincided.

With the advent of focusing telescopes, different methods have been adopted to evaluate ν_{in}. For example, with *XMM-Newton* [24] ν_{in} was obtained from the count rate measured by the portion of the focal plane position sensitive detector not exposed to the sky (out-FOV), while with the *ASCA* GIS detector [22] and with the *BeppoSAX* LECS and MECS, ν_{in} was obtained from the count rate measured during Earth pointings (*Earth pointing method*). The Earth pointing method was also adopted with the *Rossi-XTE* PCA detector [26]. The advantage of the last method is that, for the direct-viewing detectors, it does not require a variable instrument configuration while, in the case of focusing telescopes, the same portion of focal plane detector is used to estimate ν_B and ν_{in}. Furthermore, the radiation environment is not expected to change by pointing the sky or the Earth if both measurements are performed at a similar cutoff rigidity and at similar time distance from the SAGA passage. The only effect is, for a sky pointing, a background level $\nu_B^{sky} = \nu_{in} + \nu_{\mathrm{CXB}}$, while, for an Earth pointing, $\nu_B^{Earth} = \nu_{in} + \nu_A$, where ν_A is the X–ray terrestrial albedo entering through the aperture. At least for photon energies $>$15 keV, the albedo radiation cannot be neglected.

For our measurement of the unresolved CXB we have adopted the Earth pointing method, therefore the difference D between the count rate measured during blank sky field observations and that measured during Earth observations is given by

$$D = (\nu_{\rm CXB} - \nu_A) + (\nu_{in}^{sky} - \nu_{in}^{Earth}) \quad .$$

Various precautions have been taken to make $\nu_{in}^{sky} = \nu_{in}^{Earth}$. First of all, we used only the dark Earth pointings. Secondly, we separately derived D for the ON-source and OFF-source collimator positions. Indeed we found a slight difference between ON and OFF sky blank field spectra [41]. In addition, the difference D was derived only for Observation Periods (OPs) during which the corresponding ν_B^{sky} and ν_B^{Earth} were measured at similar mean values of the cutoff rigidity. Indeed, we have found that the instrument background shows intensity variations on short ($\sim$hr) and long ($\sim$yr) time scales, with the former ($\leq$15%) anti-correlated with the cutoff rigidity, while the latter ($\leq$10%), strictly correlated with the altitude of the orbit. The short time variations did not affect the spectral shape, while the long time variations did (Orlandini et al., in preparation). To satisfy the last criterion only OPs longer than 10 ks were considered. For the Earth pointings, we selected only those with the PDS axis well below the Earth limb.

Great care was devoted to the selection of blank sky fields. We discarded those pointings within 15° from the Galactic plane, in order to avoid contamination from the population of bright Galactic sources and from the Galactic diffuse emission. The complete list of the selected fields can be found elsewhere [41]. In addition, for the OFF-source pointings we filtered out those observations for which the +OFF and −OFF fields could be contaminated, e.g., from serendipitous X–ray sources, fast transients or solar flares. This selection was done by excluding from the sample those observations for which the difference between the two offset spectra was inconsistent with zero at 98% confidence level. Finally, for the ON–source pointings we accepted only those fields with the ON-source 15–50 keV net count rates (obtained by subtracting from the ON-source count rate that measured at either +OFF–source and −OFF–source) are consistent with zero within 1σ, and for which a fit with a null constant to the difference between the corresponding offset spectra gives a χ^2 per degree of freedom in the range 0.8–1.2. All the sky observations were done only when the instrument axis pointed at a direction at least 5° away from the Earth limb.

4. RESULTS

4.1. Unresolved CXB

From the whole set of 868 *BeppoSAX* observations above the galactic plane, once all the selection criteria have been taken into account, the number of valid OPs for the unresolved CXB measurement is 172. The corresponding useful observing time is 2350 ks for the ON–source observations, and 1680 ks for ±OFF–source pointings. The dark Earth was observed for a total time of 2056 ks.

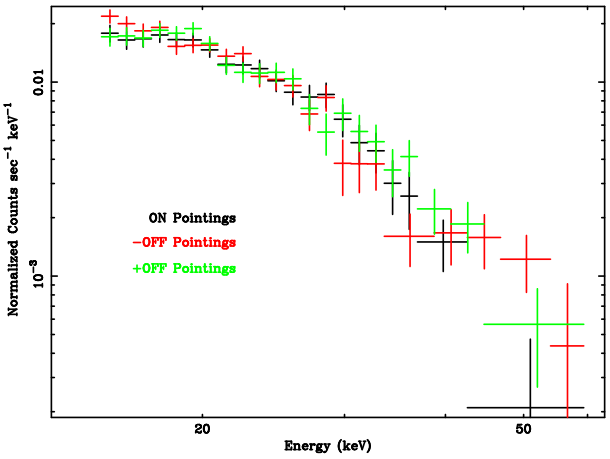

Figure 2. Difference spectrum D obtained from the ON-source and OFF-source pointings.

The obtained average difference spectra D for ON–source, +OFF–source, and −OFF–source pointings are shown in Fig. 2. As can be seen, the ON–source and OFF–source D spectra are consistent with each other, within their uncertainties. Thus we concentrated on the mean D spectrum, which is well determined up to 50 keV. For the model fitting the spectrum was rebinned following the standard criteria of having a sufficient number of counts/channel and not oversampling the instrument energy resolution.

As discussed above, the D spectrum gives the difference $\nu_{\rm CXB} - \nu_A$. Thus we fit D with the difference of two model spectra, one describing the unresolved CXB spectrum and the other describing the terrestrial albedo.

As far as the albedo spectrum is concerned, its shape is investigated since the late 1960s [see, e.g., 42, 43]. There is a general agreement [43, 44, 45] that above 40–50 keV, specially at low latitudes, it is consistent with a PL with photon index $\Gamma_A \approx 1.4$, while below it shows a flattening with a definitive low energy cutoff below 30 keV, consistent with a self-absorption of the radiation emitted from deeper and deeper atmospheric layers.

On the basis of these results, we have assumed as input model for the albedo spectrum a photoelectrically absorbed PL. In order to quantify the amount of absorption that produced the observed cutoff, we developed an atmospheric absorption model within the XSPEC software package [46], that we adopted for our model fitting. The model makes use of a grid of values of air mass X–ray attenuation coefficients as a function of the photon energy [47].

The D count rate spectrum was thus fit with the difference of an input model spectrum for the unresolved CXB and a photoelectrically absorbed PL for the albedo. For the model fit we used XSPEC v11.2. All the reported uncertainties are single parameter errors at 90% confidence

level. The deconvolved intensities per unit solid angle have been obtained by taking into account the PDS total geometric factor $G = 0.295$ cm^2 sr.

In order to decrease the number of free parameters in the fit we fixed the value of the albedo PL photon index Γ_A to 1.39 [42, 44], but we varied it in the range 1.2–2.0 in different fits finding that these changes do not significantly affect the CXB spectrum parameters. We also fixed the atmospheric depth to 2.0 g cm^{-2}, but also in this case we found no significant effect on the CXB spectral parameters if this value is varied in the range 1–6 g cm^{-2}. For the CXB we used as input model a PL, a BKNPL and a CUTOFFPL model, with the best fit results reported in Table 1, after correction for the normalization factor $R(\mathrm{PDS/MECS})$. All these laws fit the data. In the case of a PL its parameters can be constrained. In the case of a CUTOFFPL model ($\propto E^{-\Gamma}\exp(-E/E_\mathrm{c})$), which was used to describe the *HEAO–1* data (G99), the value of E_c is unconstrained and we assume the value reported by G99. In the case of a BKNPL model, even fixing the low energy photon index Γ_low to the value (1.40) obtained with all the lower energy measurements [20, 21, 22, 23, 24, 25], the other parameters could not be well constrained. Only by freezing also the break energy E_b it was possible to constrain the high energy photon index and the normalization. In order to determine the most likely value of E_b we changed it in different fits, finding that 18 keV gives the minimum χ^2. With this value frozen, the other best fit parameters are reported in Table 1.

4.2. The contribution of resolved sources

As discussed above, the unresolved CXB spectrum was obtained from properly selected ON– and OFF–source blank sky fields. While most of the ON–source fields were pointed observations of specific targets, all the selected OFF–source fields were expected to be blank fields. Instead in 33 of them (for a total exposure of 432.8 ks) we detected significant count excesses (in the range 2.5–7σ) in 15–100 keV, with a weighted mean value of their PL photon indices of 1.65 ± 0.20 and an energy flux in the range (1.4–20)$\times 10^{-12}$ erg cm^{-2} s^{-1}, corresponding to 0.1–1.5 mCrab. We found that, taking into account these excesses, the CXB intensity is increased by 4.7%. The contribution of stronger sources [see, e.g., 48] does not significantly change this figure.

4.3. The derived Earth albedo and CXB spectra

In Fig. 3 we show the derived albedo spectrum compared with the albedo spectra obtained with the *OSO III* satellite [44] and with the low–altitude polar–orbiting satellite 1972–076B [45]. As can be seen, the derived albedo spectrum is located between the *OSO III* results and the spectrum derived by Imhof et al. [45].

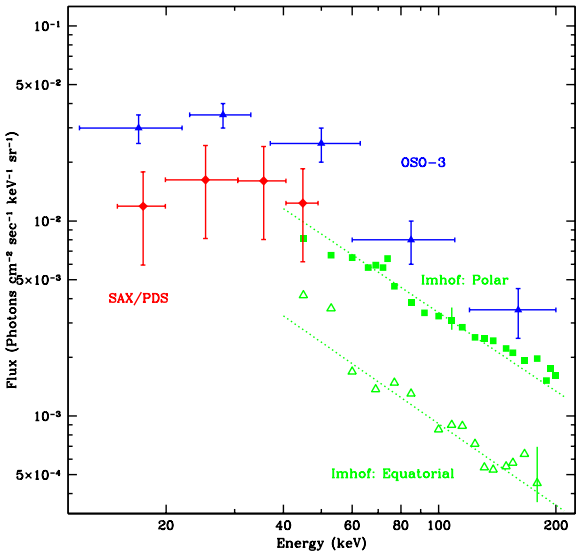

Figure 3. Comparison of the best fit albedo photon spectrum as derived by the PDS measurement (red points) with the results found by Schwartz and Peterson (1974, OSO–3 *satellite, blue points) and by Imhof et al. (1976,* 1972–076B *satellite, green points).*

In Fig. 4 we show the photon spectrum of the total CXB in the case of a modeling with a CUTOFFPL, and compare it with the most relevant results obtained thus far. As it can be seen, our measurement result is consistent with those derived with that of *HEAO–1*. A more detailed analysis of our data along with the final results and their astrophysical consequences are discussed elsewhere [49].

5. CONCLUSIONS

We can state that at present it appears unjustified the renormalization of the CXB intensity level measured with *HEAO–1* A2 and A4 by a factor of ~ 1.3 adopted in current CXB synthesis models [e.g., 8, 33]. Thus also the expectations of these models, like the role of heavily obscured AGNs ($N_\mathrm{H} > 10^{24}$ cm^{-2}, [33, 8]) or the prediction of a new population of sources with a peculiar hard X–ray spectrum [8] should be reconsidered in the light of the present results.

REFERENCES

[1] R. Giacconi, H. Gursky, F. Paolini, and B. Rossi. Evidence for X–rays from Sources outside the Solar System. 1962, *Phys. Rev. Lett.* 9, 439

[2] G. Hasinger, R. Burg, R. Giacconi, M. Schmidt, J. Trumper, and G. Zamorani. The ROSAT Deep Survey. I. X–ray Sources in the Lockman Field. 1998, *A&A* 329, 482

Table 1. Results of the spectral fits to the average difference spectrum D. In square brackets we list the parameters frozen in the fit. $I_{\rm CXB}^{\rm unres}$(20 keV) and $I_{\rm A}$(20 keV) are the unresolved CXB and albedo intensities at 20 keV, respectively. The value of 18 keV for the $E_{\rm b}$ energy was determined by minimizing the χ^2 of the fit while varying all the other parameters. The CUTOFFPL *model ($\propto E^{-\Gamma}\exp(-E/E_{\rm c})$) was used by Gruber et al. [18] to fit the* HEAO–1 *data. Because of our limited energy band we were not able to constrain $E_{\rm c}$, therefore we fixed it at the value reported by Gruber et al. [18]. Quoted errors are at 90% confidence level for a single parameter.*

	$I_{\rm CXB}^{\rm unres}$(20 keV)[a]	$I_{\rm A}$(20 keV)[a]	$\Gamma_{\rm CXB}$	$\Gamma_{\rm A}$	$\Gamma_{\rm low}$	$E_{\rm b}$ or $E_{\rm c}$ [b]	χ^2/ν
Power law	$0.098^{+0.012}_{-0.010}$	0.038 ± 0.019	$1.79^{+0.39}_{-0.35}$	[1.39]			11.7/22
Broken power law	$0.102^{+0.007}_{-0.004}$	$0.030^{+0.030}_{-0.019}$	2.1 ± 0.6	[1.39]	[1.40]	[18]	10.4/22
Cutoff power law	$0.092^{+0.010}_{-0.007}$	$0.019^{+0.019}_{-0.008}$	$1.47^{+0.35}_{-0.43}$	[1.39]		[41.13]	8.95/22

[a] In units of photons cm^{-2} s^{-1} keV^{-1} sr^{-1}

[b] In units of keV

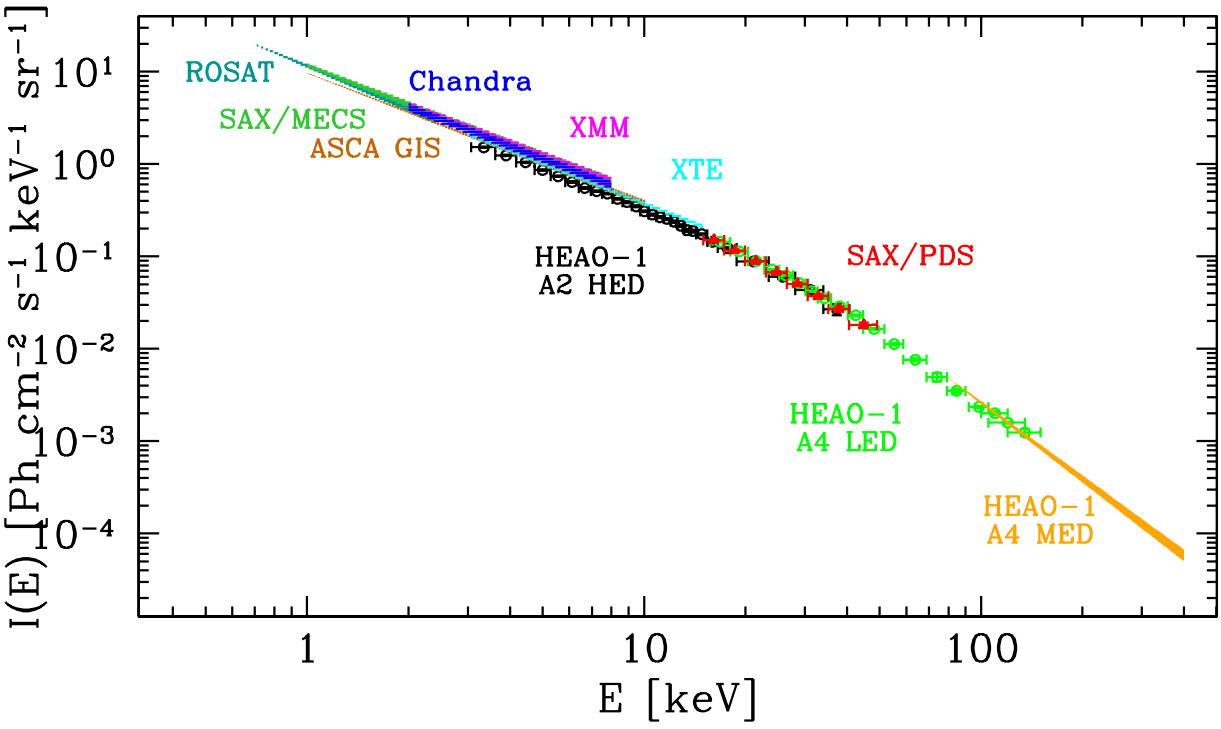

Figure 4. Total (unresolved plus resolved) CXB photon spectrum as observed with the PDS experiment (red points) compared with measurement results obtained with other missions. The CXB spectrum is modeled with a CUTOFFPL *with $E_{\rm c}$ fixed at the value of 41.13 keV quoted by Gruber et al. [18] with* HEAO–1.

[3] G. Hasinger, B. Altieri, M. Arnaud, X. Barcons, J. Bergeron, H. Brunner, M. Dadina, K. Dennerl, P. Ferrando, A. Finoguenov, R. E. Griffiths, Y. Hashimoto, F. A. Jansen, D. H. Lumb, K. O. Mason, S. Mateos, R. G. McMahon, T. Miyaji, F. Paerels, M. J. Page, A. F. Ptak, T. P. Sasseen, N. Schartel, G. P. Szokoly, J. Trümper, M. Turner, R. S. Warwick, and M. G. Watson. XMM-Newton Observation of the Lockman Hole. I. The X–ray Data. 2001, *A&A* 365, L45

[4] R. Giacconi, A. Zirm, J. Wang, P. Rosati, M. Nonino, P. Tozzi, R. Gilli, V. Mainieri, G. Hasinger, L. Kewley, J. Bergeron, S. Borgani, R. Gilmozzi, N. Grogin, A. Koekemoer, E. Schreier, W. Zheng, and C. Norman. Chandra Deep Field South: The 1 Ms Catalog. 2002, *ApJS* 139, 369

[5] A. Moretti, D. Lazzati, S. Campana, and G. Tagliaferri. The Brera Multiscale Wavelet Detection Algorithm Applied to the Chandra Deep Field-South: Deeper and Deeper. 2002, *ApJ* 570, 502

[6] D. M. Alexander, F. E. Bauer, W. N. Brandt, D. P. Schneider, A. E. Hornschemeier, C. Vignali, A. J. Barger, P. S. Broos, L. L. Cowie, G. P. Garmire, L. K. Townsley, M. W. Bautz, G. Chartas, and W. L. W. Sargent. The Chandra Deep Field North Survey. XIII. 2 Ms Point-Source Catalogs. 2003, *AJ* 126, 539

[7] R. C. Hickox and M. Markevitch. Absolute Measurement of the Unresolved Cosmic X–ray Background in the 0.5-8 keV Band with Chandra. 2006, *ApJ* 645, 95

[8] A. Comastri. The Missing X–ray Background. In R. Mujica and R. Maiolino, editors, *Multiwavelength AGN Surveys*, page 323. Singapore: World Scientific Publishing Company, 2004.

[9] H. M. Horstman, G. Cavallo, and E. Moretti-Horstman. The X and Gamma Diffuse Background. 1975, *Rivista Nuovo Cimento* 5, 255

[10] F. E. Marshall, E. A. Boldt, S. S. Holt, R. B. Miller, R. F. Mushotzky, L. A. Rose, R. E. Rothschild, and P. J. Serlemitsos. The Diffuse X–ray Background Spectrum from 3 to 50 keV. 1980, *ApJ* 235, 4

[11] E. Boldt. The Cosmic X–ray Background. 1987, *Phys. Rep.* 146, 215

[12] E. Boldt. The X–Ray LogN-LogS Relation. In Y. Tanaka, editor, *Physics of Neutron Stars and Black Holes*, page 342. Tokio: Universal Academy, 1988.

[13] E. Boldt. Is AGN Spectral Evolution Needed for the CXB? In *X–ray Astronomy*, volume SP–296, page 797. Noordwijk: ESTEC, 1989.

[14] E. Boldt. The AGN contribution to the X–ray background. In X. Barcons and A.C. Fabian, editors, *The X–ray Background*, page 149. Cambride: Cambridge University Press, 1992.

[15] J. C. Mather, E. S. Cheng, R. E. Eplee, R. B. Isaacman, S. S. Meyer, R. A. Shafer, R. Weiss, E. L. Wright, C. L. Bennett, N. W. Boggess, E. Dwek, S. Gulkis, M. G. Hauser, M. Janssen, T. Kelsall, P. M. Lubin, S. H. Moseley, T. L. Murdock, R. F. Silverberg, G. F. Smoot, and D. T. Wilkinson. A Preliminary Measurement of the Cosmic Microwave Background Spectrum by the Cosmic Background Explorer (COBE) Satellite. 1990, *ApJ* 354, L37

[16] R. E. Rothschild, W. A. Baity, D. E. Gruber, J. L. Matteson, L. E. Peterson, and R. F. Mushotzky. 2–165 keV Observations of Active Galaxies and the Diffuse Background. 1983, *ApJ* 269, 423

[17] D. E. Gruber. The Hard X–ray Background. In X. Barcons and A.C. Fabian, editors, *The X–ray Background*, page 44. (Cambridge: Cambridge University Press), 1992.

[18] D. E. Gruber, J. L. Matteson, L. E. Peterson, and G. V. Jung. The Spectrum of Diffuse Cosmic Hard X–Rays Measured with HEAO 1. 1999, *ApJ* 520, 124

[19] R. L. Kinzer, G. V. Jung, D. E. Gruber, J. L. Matteson, and L. E. Peterson. Diffuse Cosmic Gamma Radiation Measured by HEAO 1. 1997, *ApJ* 475, 361

[20] I. Georgantopoulos, G. C. Stewart, T. Shanks, B. J. Boyle, and R. E. Griffiths. A Deep ROSAT Survey — V. The Extragalactic Populations at Faint Fluxes. 1996, *MNRAS* 280, 276

[21] K. C. Gendreau, R. Mushotzky, A. C. Fabian, S. S. Holt, T. Kii, P. J. Serlemitsos, Y. Ogasaka, Y. Tanaka, M. W. Bautz, Y. Fukazawa, Y. Ishisaki, Y. Kohmura, K. Makishima, M. Tashiro, Y. Tsusaka, H. Kunieda, G. R. Ricker, and R. K. Vanderspek. ASCA Observations of the Spectrum of the X–Ray Background. 1995, *PASJ* 47, L5

[22] A. Kushino, Y. Ishisaki, U. Morita, N. Y. Yamasaki, M. Ishida, T. Ohashi, and Y. Ueda. Study of the X–Ray Background Spectrum and Its Large-Scale Fluctuation with ASCA. 2002, *PASJ* 54, 327

[23] A. Vecchi, S. Molendi, M. Guainazzi, F. Fiore, and A. N. Parmar. The BeppoSAX 1–8 keV Cosmic Background Spectrum. 1999, *A&A* 349, L73

[24] D. H. Lumb, R. S. Warwick, M. Page, and A. De Luca. X–ray Background Measurements with XMM-Newton EPIC. 2002, *A&A* 389, 93

[25] A. De Luca and S. Molendi. The 2–8 keV Cosmic X–ray Background Spectrum as Observed with XMM-Newton. 2004, *A&A* 419, 837

[26] M. Revnivtsev, M. Gilfanov, R. Sunyaev, K. Jahoda, and C. Markwardt. The Spectrum of the Cosmic X–ray Background Observed by RTXE/PCA. 2003, *A&A* 411, 329

[27] M. V. Zombeck. *Handbook of Space Astronomy and Astrophysics*. Cambridge University Press, 1990.

[28] M. Revnivtsev, M. Gilfanov, K. Jahoda, and R. Sunyaev. Intensity of the Cosmic X–ray Backgound from HEAO1/A2 Experiment. 2005, *A&A* 444, 381

[29] K. Jahoda et al. 2006, in preparation (available online at http://lheawww.gsfc.nasa.gov/users/keith/a2_cxb_15dec2005.pdf).

[30] D. McCammon, D. N. Burrows, W. T. Sanders, and W. L. Kraushaar. The soft X–ray diffuse background. 1983, *ApJ* 269, 107

[31] M. A. Worsley, A. C. Fabian, X. Barcons, S. Mateos, G. Hasinger, S. Mateos, and H. Brunner. The (un)resolved X–ray Background in the Lockman Hole. 2004, *MNRAS* 352, L28

[32] M. A. Worsley, A. C. Fabian, F. E. Bauer, D. M. Alexander, G. Hasinger, S. Mateos, H. Brunner, W. N. Brandt, and D. P. Schneider. The unresolved hard X-ray background: the missing source population implied by the Chandra and XMM-Newton deep fields. 2005, *MNRAS* 357, 1281

[33] Y. Ueda, M. Akiyama, K. Ohta, and T. Miyaji. Cosmological Evolution of the Hard X–Ray Active Galactic Nucleus Luminosity Function and the Origin of the Hard X–Ray Background. 2003, *ApJ* 598, 886

[34] F. Frontera, E. Costa, D. dal Fiume, M. Feroci, L. Nicastro, M. Orlandini, E. Palazzi, and G. Zavattini. The High Energy Instrument PDS on-board the BeppoSAX X–ray Astronomy Satellite. 1997, *A&AS* 122, 357

[35] R. Jager, W. A. Mels, A. C. Brinkman, M. Y. Galama, H. Goulooze, J. Heise, P. Lowes, J. M. Muller, A. Naber, A. Rook, R. Schuurhof, J. J. Schuurmans, and G. Wiersma. The Wide Field Cameras onboard the BeppoSAX X–ray Astronomy Satellite. 1997, *A&AS* 125, 557

[36] F. Frontera. X–Ray Observations of Gamma-Ray Burst Afterglows. In K. Weiler, editor, *Supernovae and Gamma Ray Bursters*, page 317. (Berlin: Springer), 2003. Lecture Notes in Physics, Vol. 598.

[37] F. Frontera, E. Costa, D. Dal Fiume, M. Feroci, L. Nicastro, M. Orlandini, E. Palazzi, and G. Zavattini. PDS Experiment on board the BeppoSAX Satellite: Design and in-flight Performance Results. 1997, *Proc. SPIE* 3114, 206

[38] L. M. Bartlett. *High Resolution Gamma-ray Spectroscopy of the Crab*. PhD thesis, NASA/Goddard Space Flight Center, 1994.

[39] R. Willingale, B. Aschenbach, R. G. Griffiths, S. Sembay, R. S. Warwick, W. Becker, A. F. Abbey, and J.-M. Bonnet-Bidaud. New Light on the X–ray Spectrum of the Crab Nebula. 2001, *A&A* 365, L212

[40] A. Toor and F. D. Seward. The Crab Nebula as a Calibration Source for X–ray Astronomy. 1974, *AJ* 79, 995

[41] R. Landi. *The Hard X–ray Sky off the Galactic Plane as seen by the BeppoSAX/PDS Experiment*. PhD thesis, Physics Department, University of Bologna, 2005.

[42] J. L. Peterson, D. A. Schwartz, and J. C. Ling. Spectrum of Atmospheric Gamma Rays to 10 MeV at $\lambda = 40^{\circ}$. 1973, *J. Geophys. Res.* 78, 7942

[43] L. E. Peterson. Instrumental Technique in X–ray Astronomy. 1975, *ARA&A* 13, 423

[44] D. A. Schwartz and L. E. Peterson. The Spectrum of Diffuse Cosmic X–Rays Observed by OSO–3 Between 7 and 100 KEV. 1974, *ApJ* 190, 297

[45] W. L. Imhof, G. H. Nakano, and J. B. Reagan. High-resolution Measurements of Atmospheric Gamma Rays from a Satellite. 1976, *J. Geophys. Res.* 81, 2835

[46] K. A. Arnaud. XSPEC: The First Ten Years. 1996, *ASP Conf. Series* 101, 17

[47] J. H. Hubbell and S. M. Seltzer, 1996. available online at http://physics.nist.gov/PhysRefData/XrayMassCoef/cover.html.

[48] R. Krivonos, A. Vikhlinin, E. Churazov, A. Lutovinov, S. Molkov, and R. Sunyaev. Extragalactic Source Counts in the 20–50 keV Energy Band from the Deep Observation of the Coma Region by INTEGRAL IBIS. 2005, *ApJ* 625, 89

[49] F. Frontera, M. Orlandini, R. Landi, A. Comastri, F. Fiore, G. Setti, L. Amati, E. Costa, N. Masetti, and E. Palazzi. The cosmic X–ray background and the population of the most heavily obscured AGNs *ApJ*, 2006. submitted (astro-ph/0611228).